Fabrication of high-critical current density $YBa_2Cu_3O_{7-\delta}$ films using a fluorine-free sol gel approach

Y. Xu
Oak Ridge National Laboratory, Oak Ridge, Tennessee 37831, and Department of Materials Science and Engineering, University of Cincinnati, Cincinnati, Ohio 45221

A. Goyal[a] and N.A. Rutter
Oak Ridge National Laboratory, Oak Ridge, Tennessee 37831

D. Shi
Department of Materials Science and Engineering, University of Cincinnati, Cincinnati, Ohio 45221

M. Paranthaman, S. Sathyamurthy, P.M. Martin, and D.M. Kroeger
Oak Ridge National Laboratory, Oak Ridge, Tennessee 37831

(Received 2 October 2002; accepted 13 December 2002)

Superconducting $YBa_2Cu_3O_{7-\delta}$ (YBCO) films with critical transition temperature $T_c(0)$ of 90 K were fabricated via a fluorine-free, metal trimethylacetate based sol-gel route. Precursor films were spin-coated onto single-crystal (001) $LaAlO_3$ (LAO) and (001) $SrTiO_3$ (STO) substrates. Optimization of the burnout process resulted in films with excellent out-of-plane and in-plane texture. Transport critical current densities, J_c, of 1.6 and 1.1 MA/cm^2 were obtained at 77 K in self-field on films grown on LAO and STO substrates, respectively. This is the first demonstration of high-J_c YBCO film fabrication using a fluorine-free, *ex-situ* process.

I. INTRODUCTION

Chemical solution deposition (CSD) is one of the deposition techniques used to fabricate $YBa_2Cu_3O_{7-\delta}$ (YBCO) films. The method of CSD has some advantages over vapor deposition, such as precise control of composition, high speed, and low cost. Metalorganic deposition (MOD), one of the popular CSD methods, involves the coating of metalorganic precursor solution on a substrate followed by thermal decomposition to form the final desired compound. Epitaxial nucleation and growth can occur when the process is carried out on lattice matched single-crystal substrates. Trifluoroacetate (TFA) MOD is well established as a promising method for the fabrication of high-critical current density (high-J_c) (over 1 MA/cm^2) YBCO films[1,2] and has been applied[3] on biaxially textured metal substrates like rolling assisted biaxially textured substrates.[4,5–7] The interest in fluorine-containing precursors for YBCO arises because it is believed that non-fluorine precursors might result in the formation of stable $BaCO_3$ at the grain boundaries.[8] The use of trifluoroacetate salts appears to avoid the formation of $BaCO_3$ because the stability of barium fluoride is greater than that of barium carbonate and fluorine can be removed during the high-temperature anneal (>650 °C) in a humid, low-oxygen, partial pressure environment.[2] Nevertheless, several factors maintain interest in a fluorine-free precursor MOD approach, the most important being that removal of fluorine in the form of HF at high temperatures is a nontrivial process. There appear to be many issues related to fluid flow and complicated reactor designs may be required for scaleup. Furthermore, a recent overview of previous attempts at YBCO film fabrication using non-fluorine-based bulk solution techniques finds no previous report of high-J_c film fabrication using fluorine-free precursors.[9] In this work, we report on the fabrication of high-quality YBCO films using a fluorine-free precursor. The transport J_c of these films is more than 1 MA/cm^2 at 77 K and self-field.

II. EXPERIMENTAL

Films were prepared by the following procedure: $Y(NO_3)_3 \cdot 4H_2O$ (Alfa Aesar, Ward Hill, MA) and $Cu(NO_3)_3 \cdot 2.5H_2O$ (Alfa Aesar) were reacted with $NH_4(C_4H_9COO)$ at room temperature for about 30 min, respectively, to form $Y(C_4H_9COO)_3$ (yttrium trimethylacetate) and $Cu(C_4H_9COO)_2$ (copper trimethylacetate); then, $Ba(OH)_2 \cdot 8H_2O$ (Alfa Aesar), $Y(C_4H_9COO)_3$, and $Cu(C_4H_9COO)_2$ were dissolved in propionic acid (PP) at room temperature in the stoichiometry Y:Ba:Cu of 1:2:3 and amylamine (AM) was added to the solution in the

[a]Address all correspondence to this author at Bethel Valley Road, P.O. Box 2008 Oak Ridge, TN 37831-6116.
e-mail: goyala@ornl.gov

ratio PP:AM = 4:3 to form a dark green solution with a total ionic concentration of 0.5–0.8 M. After filtration, this solution was coated on the substrates using a spin-coater at a speed of 2000–5000 rpm at room temperature. Films were then subjected to a burnout anneal in O_2 bubbled through water with a dew point of 45 °C at temperatures of either 310, 400, 500, or 600 °C. Then films were given a high-temperature anneal by heat-up to 745 °C at 40 °C/min for 1 h in a low oxygen partial pressure [$P(O_2)$ = 180 ppm]. The flowing gas was bubbled through water with a dew point of 45 °C during the heating-up and high-temperature dwell as well. Dry gas was used for the last 15 min of the anneal. For oxygenation, the films were held at 500 °C for 30 min followed by furnace cooling to room temperature in flowing oxygen. The J_c was measured in the usual four-point transport method at 77 K and zero field. In addition, textures were analyzed by x-ray diffraction (XRD); surface morphology was observed by scanning electron microscopy (SEM). To examine the composition of the sample after burnout and anneal, Rutherford backscattering spectroscopy (RBS) was performed using a 5.0 MeV He^{2+} ion beam with a back-scatter angle of 160°. The thickness of the film was measured using RBS and also by cross-section transmission electron microscopy (TEM). TEM results showed that the thickness of the films was in the range of 70–100 nm; hence, an average value of 85 nm was used as the film thickness.

III. RESULTS AND DISCUSSION

The dependence of J_cs on burnout temperatures is shown in Table I. The J_c values are strongly related to the burnout temperature. The highest J_c values on both $LaAlO_3$ (LAO) and $SrTiO_3$ (STO) substrates were obtained for films burnout at 400 °C. For other temperatures, J_c is one or two orders of magnitude lower than the optimum values.

To calibrate the composition and thickness precisely in RBS measurements, YBCO films were fabricated on MgO substrates and treated with the same condition as those of YBCO films on LAO and STO substrates. The RBS results (Fig. 1) show that the ratio of Y:Ba:Cu is 1:2:3 both for the burnout samples and for the high temperature annealed samples. One difference that can be identified easily in the RBS data is that spectra of barium tend to be wider because of barium diffusion at high temperatures. In both cases, there is no evidence of loss of copper during the burnout and high temperature anneal processes.

Good texture is critical for the transport of current in high-temperature superconductors. Figure 2 shows the θ–2θ scan of YBCO on an LAO substrate burnout at 400 °C followed by 745 °C anneal for 1 h. Only (00*l*)

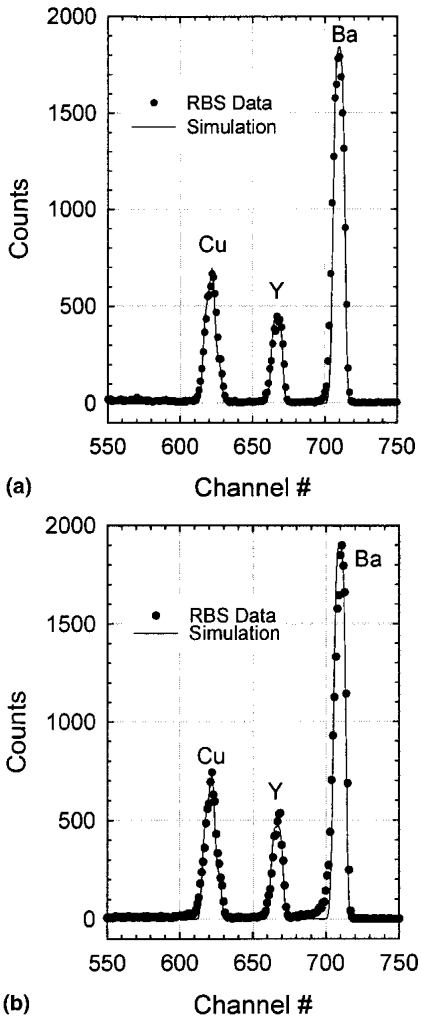

FIG. 1. (a) RBS data for YBCO film for 400 °C burnout in wet oxygen and (b) RBS spectra after 740 °C anneal in 180 ppm oxygen partial pressure and wet furnace gas.

TABLE I. Critical current density, J_c, of YBCO versus burnout temperature on LAO and STO substrates [annealed at 745 °C/1 h in humid Ar/O_2 atmosphere with $P(O_2)$ = 180 ppm].

	Transport J_c (MA/cm^2), for various burnout temperatures (°C)			
Substrates	310	400	500	600
LAO	0.04	1.65	0.15	<0.01
STO	0.06	1.10	0.11	0.04

YBCO peaks are seen. No $BaCO_3$ is observed in XRD. Cross-section TEM analysis confirm no $BaCO_3$ was present in the film.[10] Rocking curve were performed on YBCO films with different burnout temperatures. The highest intensity, shown in the rocking curves in Fig. 3, was obtained on the sample burnout at 400 °C, followed by the samples burnout at 310 and 500 °C, and the lowest is the sample burnout at 600 °C. The intensity variation is an indication of the crystallinity of the film, the completeness of the conversion to YBCO, and of the degree of epitaxy of the film with respect to the substrate. The values of full width at half maximum (FWHM), shown in Fig. 3, are small and nearly constant for all of the samples. YBCO (005) ω scans show that the 400 °C burnout sample has the lowest FWHM of 0.59° and the 600 °C burned sample has the highest FWHM of 0.64°. The FWHM values from (115) ϕ scans for the 400 °C burnout YBCO on LAO and STO of 1.6° and 1.3°, respectively, show good in-plane textures. XRD θ–2θ scans show that no $BaCO_3$ phase was present after reaction. Pole figures were obtained to get a more complete examination of the degree of epitaxy. The *R–T* curve inset of Fig. 3 shows a typical transition.

Figure 4 shows (115) pole figures for YBCO films grown on LAO substrates. For the 400 °C burnout sample, only four (115) peaks are seen, confirming the good in-plane (*a/b*) and out-of-plane (*c*) textures. However, for the remaining three samples, there are additional peaks. The peaks represented by "□" are from *a*-axis-oriented grains, which can also be identified in SEM morphologies shown in Fig. 6, and the peaks represented by the small circle "○" come from the *c*-axis-oriented grains. Clearly, the temperature of burnout seems to affect the final YBCO film greatly.

To further investigate the influence of the burnout temperature, the morphologies of precursor films after the burnout were studied by SEM. Figure 5 shows SEM micrographs of samples burned-out at different temperatures. It is clear that the burnout temperature affects the morphology of the film. The 400 °C burnout film shows smooth surface decorated with small holes in diameter of about 0.1–0.2 μm. On the basis of the differential thermal analysis/thermogravimetric analysis, these holes

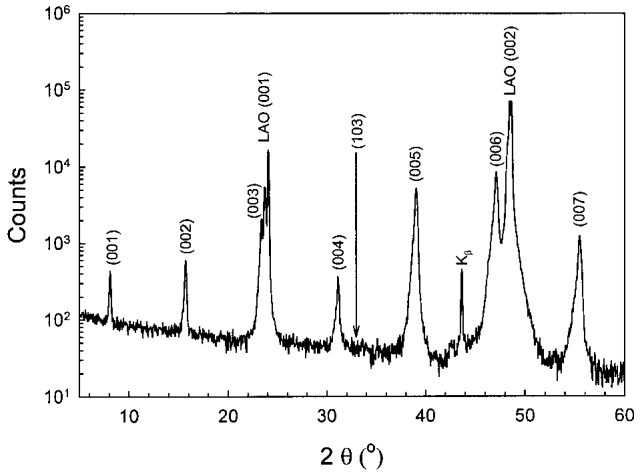

FIG. 2. X-ray θ–2θ scan of YBCO film on LAO (001) substrate burnout at 400 °C and annealed at 745 °C/1 h in humid Ar/O_2 atmosphere with $P(O_2)$ = 180 ppm.

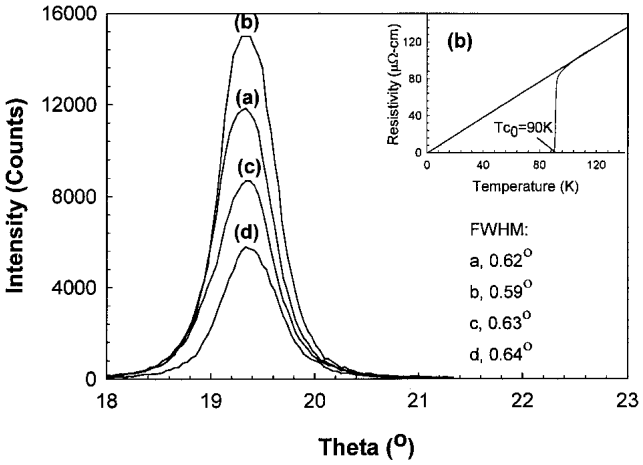

FIG. 3. The 005 ω scan of YBCO films on LAO (001) substrate burnout at different temperatures and annealed at 745 °C/1 h in humid Ar/O_2 atmosphere with $P(O_2)$ = 180 ppm: (a) 310 °C; (b) 400 °C; (c) 500 °C; (d) 600 °C. The *R–T* curve in the inset shows a typical transition.

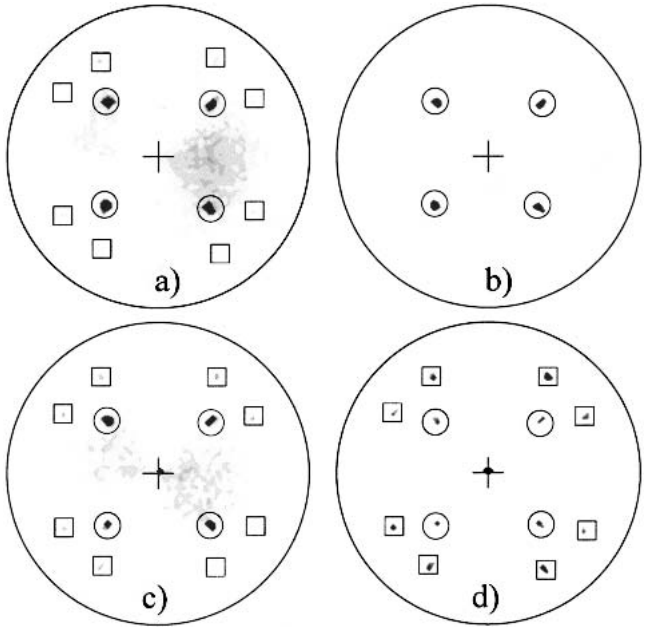

FIG. 4. YBCO (115) pole figure of films annealed at 745 °C/1 h in humid Ar/O_2 atmosphere with $P(O_2)$ = 180 ppm: (a) 310 °C burnout sample; (b) 400 °C burnout sample; (c) 500 °C burnout sample; (d) 600 °C burnout sample. Note: "○" and "□" represent different sets of orientations.

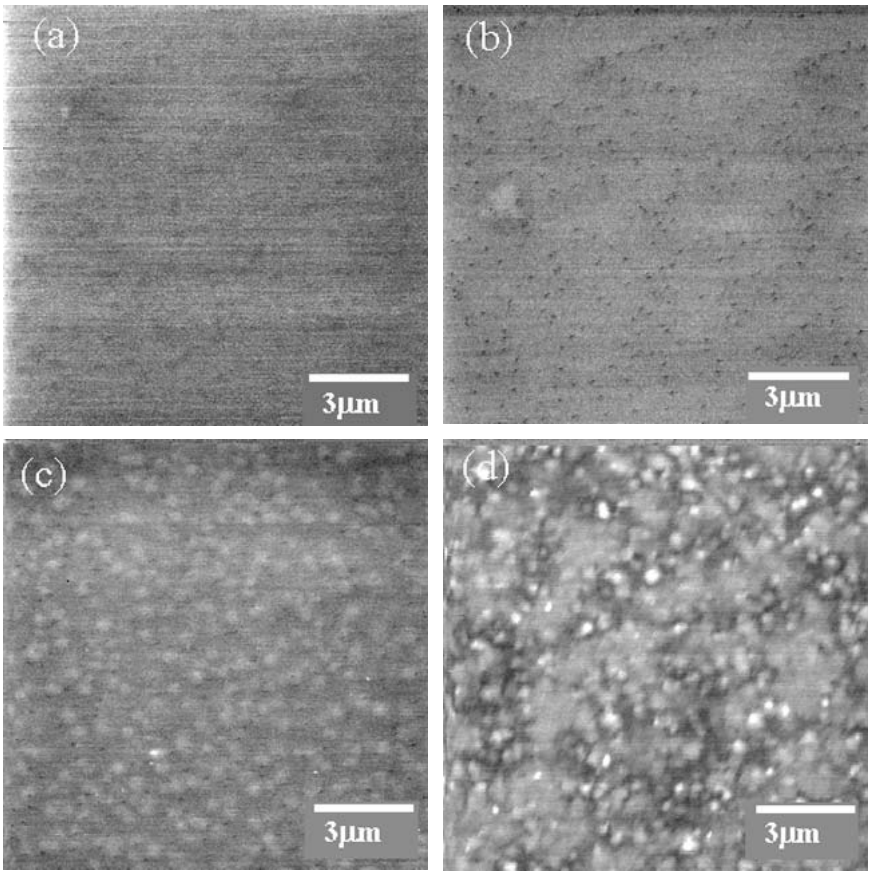

FIG. 5. SEM morphologies of YBCO films on LAO (001) substrates burnout in humid oxygen at the following temperatures: (a) 310 °C; (b) 400 °C; (c) 500 °C; (d) 580 °C.

were probably formed by a solvent evaporation and a decomposition of a copper-containing organic compound. For the sample burnout at 310 °C, an even smoother surface with fewer holes demonstrates a somewhat incomplete decomposition at this temperature. Films get rougher and more inhomogeneous with an increase in the burnout temperature.

After high-temperature anneal at 745 °C for 1 h in humid low-oxygen partial pressure, the precursor films were changed to YBCO films. The top-view SEM morphologies of these films are shown in Fig. 6. The surface morphologies of the YBCO films depend clearly on the burnout conditions, which confirm the reaction status during the burnout in oxygen. Aligned rodlike particles were observed on the surface of the 310 °C burnout sample. These rods are of YBCO phase and are slightly Cu-rich. The surface morphology of the 500 °C burnout sample [Fig. 6(c)] is relatively smooth, although large holes decorate the surface. The morphology of the 400 °C burned sample [Fig. 6(b)] is similar to those reported by Feenstra *et al.*[11] in their e-beam-derived YBCO film with a post-anneal. Enhanced growth of platelike grains and the presence of small pores were observed in films burnout at 400 °C. The absence of *a*-axis-oriented grains and few second phase particles indicate the potential for high J_c. Critical temperature (T_c) measurement (Fig. 3 inset) shows the zero resistance transition temperature is 90 K, and the extrapolation of the temperature dependence of resistivity to 0 K indicates no residual resistivity, implying a good quality of the YBCO film burnout at 400 °C. The *a*-orientated and other misoriented grains, pores, and precipitates are responsible for the low J_c of YBCO films burnout at 310, 500, and 600 °C.

IV. CONCLUSIONS

In summary, we have prepared YBCO films through a fluorine-free metal trimethylacetate–propionic acid mixed with amine based sol-gel route. A $T_c(0)$ of 90 K and a transport J_c of 1.6 MA/cm^2 (77 K and self-field) were demonstrated for the YBCO film on (001)-orientated LAO substrate prepared by 400 °C burnout followed by 745 °C anneal in 180 ppm oxygen partial pressure and humid atmosphere. Low current densities on the samples burnout at other temperatures arose from *a*-oriented grains (or other misoriented grains), poor surface morphologies, and second-phase segregations. RBS

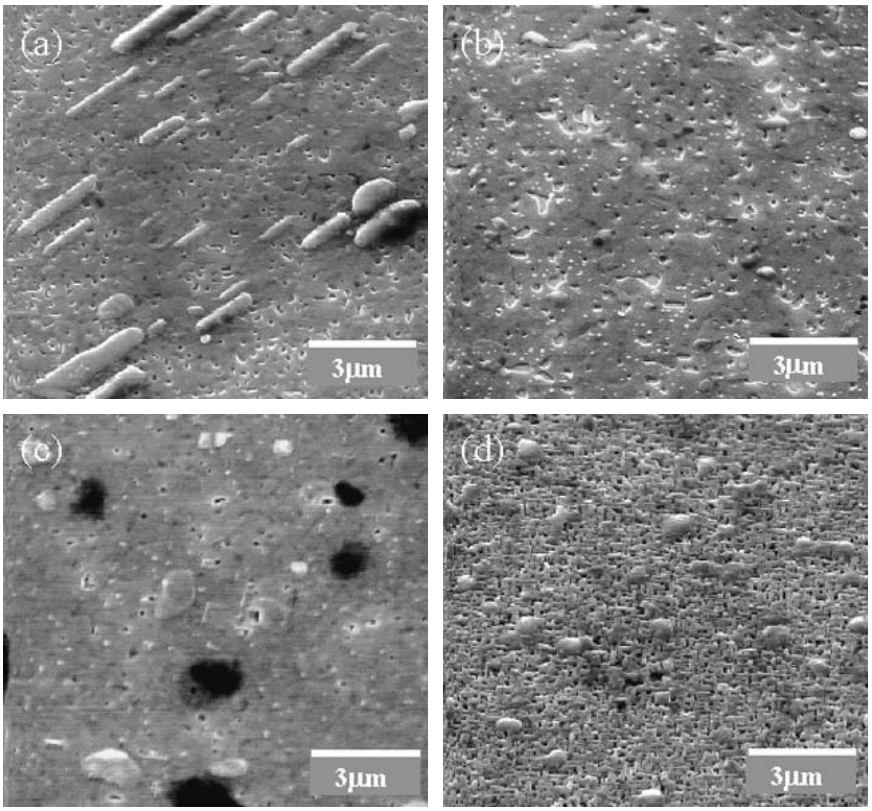

FIG. 6. SEM morphologies of YBCO films on LAO (001) substrate burnout at different temperatures and annealed at 745 °C/1 h in humid Ar/O_2 atmosphere with $P(O_2) = 180$ ppm: (a) 310 °C; (b) 400 °C; (c) 500 °C; (d) 600 °C.

data show the stoichiometry of Y:Ba:Cu is 1:2:3 both for the burnout and high temperature annealed samples; no loss of copper is observed. No $BaCO_3$ was observed in the fully processed films as determined by x-ray and TEM analysis.

ACKNOWLEDGMENTS

This work was sponsored by the United States Department of Energy (USDOE), Office of Energy Efficiency and Renewable Energy—Superconductivity Program for Electric Systems. The research was performed at the Oak Ridge National Laboratory, managed by U.T.-Battelle, LLC, for the USDOE under Contract No. DE-AC05-00OR22725.

REFERENCES

1. A. Gupta, R. Jagannathan, E.I. Cooper, E.A. Geiss, J.I. Landman, and B.W. Hussey, Appl. Phys. Lett. **52,** 2077 (1988).
2. P.C. Mclntyre, M.J. Cima, J.A. Smith, R.B. Hallock, M.P. Siegal, and J.M. Phillips, J. Appl. Phys. **71,** 1868 (1992).
3. A.P. Malozemoff, S. Annavarapu, L. Fritzemeier, Q. Li, V. Prunier, M. Rupich, C. Thieme, W. Zhang, A. Goyal, M. Paranthaman, and D.F. Lee, Supercond. Sci. Technol. **13,** 473 (2000).
4. A. Goyal, D.P. Norton, J.D. Budai, M. Paranthaman, E.D. Specht, D.M. Kroeger, D.K. Christen, Q. He, B. Saffian, F.A. List, D.F. Lee, P.M. Martin, C.E. Klaburde, E. Hartfield, and V.K. Sikka, Appl. Phys. Lett. **69,** 1795 (1996).
5. A. Goyal, J.D. Budai, D.M. Kroeger, D.P. Norton, D.P. Christen, and E.D. Specht, U.S. Patent No. 5 739 086 (14 April 1998).
6. A. Goyal, J.D. Budai, D.M. Kroeger, D.P. Norton, D.P. Christen, and E.D. Specht, U.S. Patent No. 5 741 377 (21 April 1998).
7. A. Goyal, J.D. Budai, D.M. Kroeger, D.P. Norton, D.P. Christen, and E.D. Specht, U.S. Patent No. 5 898 020 (27 April 1999).
8. F. Parmigiani, G. Chiarello, and N. Ripamonti, Phys. Rev. B **36,** 7148 (1987).
9. M. Paranthaman, in *Next Generation HTS Conductors*, edited by A. Goyal (Plenum Publishing, New York, 2002).
10. J. Lian, Y. Xu, A. Goyal, and D. Shi (to be published).
11. R. Feenstra, T.B. Lindemer, J.D, Budai, and M.D. Galloway, J. Appl. Phys. **69,** 6569 (1991).